Geophysical Research Letters

RESEARCH LETTER
10.1029/2020GL090003

Long-Term Increase in Antarctic Ice Sheet Vulnerability Driven by Bed Topography Evolution

Guy J. G. Paxman[1,2], Edward G. W. Gasson[3], Stewart S. R. Jamieson[1], Michael J. Bentley[1], and Fausto Ferraccioli[4]

[1]Department of Geography, Durham University, Durham, UK, [2]Now at Lamont-Doherty Earth Observatory, Columbia University, Palisades, NY, USA, [3]School of Geographical Sciences, University of Bristol, Bristol, UK, [4]British Antarctic Survey, Cambridge, UK

Abstract Ice sheet behavior is strongly influenced by the bed topography. However, the effect of the progressive temporal evolution of Antarctica's subglacial landscape on the sensitivity of the Antarctic Ice Sheet (AIS) to climatic and oceanic change has yet to be fully quantified. Here we investigate the evolving sensitivity of the AIS using a series of data-constrained reconstructions of Antarctic paleotopography since glacial inception at the Eocene-Oligocene transition. We use a numerical ice sheet model to subject the AIS to schematic climate and ocean warming experiments and find that bed topographic evolution causes a doubling in ice volume loss and equivalent global sea level rise. Glacial erosion is primarily responsible for enhanced ice sheet retreat via the development of increasingly low-lying and reverse sloping beds over time, particularly within near-coastal subglacial basins. We conclude that AIS sensitivity to climate and ocean forcing has been substantially amplified by long-term landscape evolution.

Plain Language Summary The Antarctic Ice Sheet is situated above a large landmass, the geometry of which is an important control on the behavior of the ice sheet and how it responds to climatic change. However, Antarctica's subglacial landscape has evolved significantly since the formation of the first ice sheets approximately 34 million years ago, which implies that the sensitivity of the ice sheet to climate change may also have changed over time. Our ice sheet model experiments show that the progressive evolution of Antarctica's bed topography has enhanced the sensitivity of the Antarctic Ice Sheet to climate and ocean warming, meaning that a greater volume of ice is lost for a given warming scenario when using the modern topography compared to past topographies. In particular, the lowering of bed elevations by glacial erosion has caused a notable increase in ice sheet sensitivity within subglacial basins close to the ice sheet margin.

Key Points:
- We investigate the influence of the progressive evolution of bed topography on the sensitivity of the Antarctic Ice Sheet to climatic change
- Bed topographic evolution since 34 Ma causes a doubling in Antarctic ice volume loss in our schematic ice sheet model experiments
- Antarctic Ice Sheet sensitivity to climate and ocean forcing has been substantially amplified by long-term landscape evolution

Supporting Information:
- Supporting Information S1

Correspondence to:
G. J. G. Paxman,
gpaxman@ldeo.columbia.edu

Citation:
Paxman, G. J. G., Gasson, E. G. W., Jamieson, S. S. R., Bentley, M. J., & Ferraccioli, F. (2020). Long-term increase in Antarctic Ice Sheet vulnerability driven by bed topography evolution. *Geophysical Research Letters*, *47*, e2020GL090003. https://doi.org/10.1029/2020GL090003

Received 27 JUL 2020
Accepted 30 SEP 2020
Accepted article online 13 OCT 2020

1. Introduction

The future behavior of the Antarctic Ice Sheet (AIS; Figure 1) in a warming climate is a key uncertainty in projecting global sea level rise over the course of the current century and beyond. The modern AIS contains a volume of ice equivalent to ~57.9 m of global sea level rise, of which ~5.30 m is located within the West Antarctic Ice Sheet (WAIS) and ~52.2 m within the East Antarctic Ice Sheet (EAIS; Figure 1) (Morlighem et al., 2020). Of major importance is the observation that ~45% of the modern-day grounded AIS flows over bed that lies below sea level, including the majority of the WAIS and approximately one third of the EAIS (Figure 1) (Fretwell et al., 2013). These regions are believed to be susceptible to dynamic marine ice sheet instability processes in locations where the bed deepens inland and the ice sheet may ultimately undergo rapid retreat (Mercer, 1978; Schoof, 2007; Thomas, 1979). Projections of the likely contributions of WAIS and EAIS retreat to global sea level rise over the coming century are derived from process-based numerical ice sheet model and range from a few centimeters to 1 m by the year 2100 (DeConto & Pollard, 2016; Edwards et al., 2019; Golledge et al., 2015).

Uncertainties in the projected rate and magnitude of future sea level change arise for two main reasons. First, different ice sheet models deploy different physical mechanics, boundary conditions, and parameterizations, in particular the model physics pertaining to the processes associated with marine instabilities such as ice shelf hydrofracture and ice cliff failure (Edwards et al., 2019; Pollard et al., 2015). Second, models are often

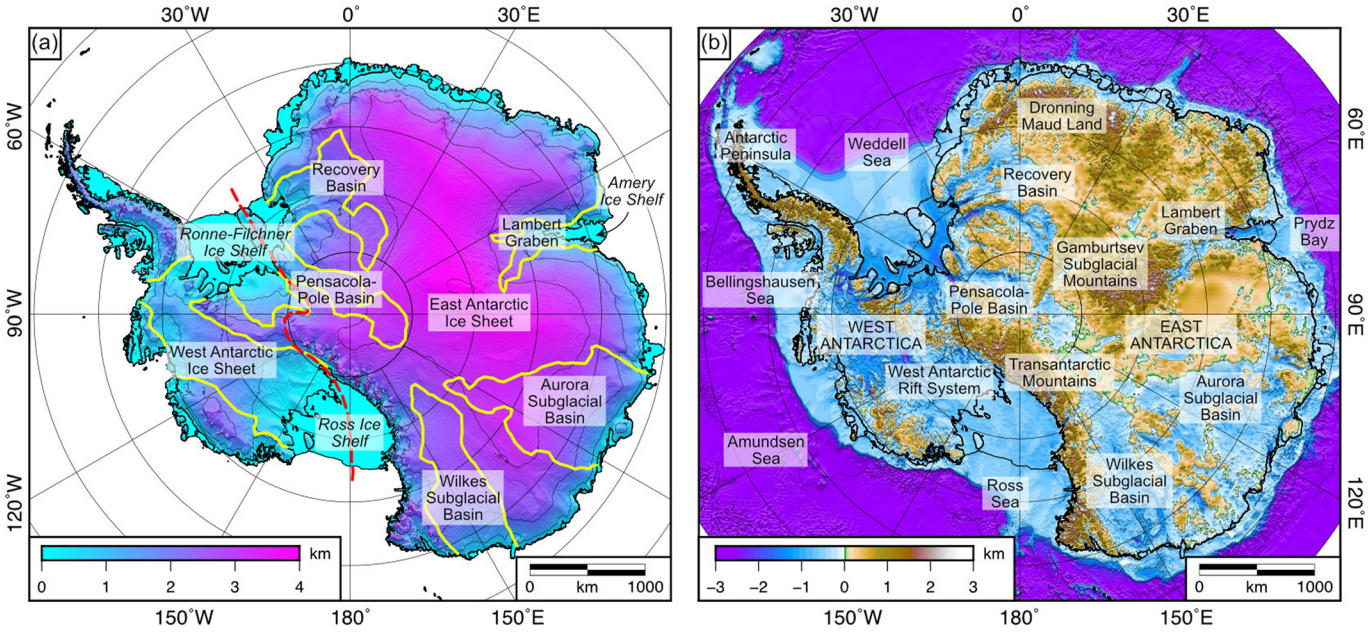

Figure 1. Present-day ice sheet surface and bed elevation of Antarctica. (a) AIS surface elevation relative to mean sea level (Slater et al., 2018). Black lines denote the modern grounding line and ice calving front. Red dashed line delineates the boundary between ice sheet drainage basins of the EAIS and the WAIS, as defined by the ice sheet mass balance intercomparison exercise (IMBIE) (Rignot et al., 2019). Yellow outlines mark areas of ice underlain by major subglacial basins situated below sea level. (b) Modern bed elevation of Antarctica relative to mean sea level (Paxman et al., 2019). The bed elevation grid is based on the Bedmap2 compilation (Fretwell et al., 2013) with the addition of more recently acquired ice thickness data in regions of previously limited coverage, such as the Pensacola-Pole Basin (Forsberg et al., 2018; Jordan et al., 2018). Approximately 45% of the bed below grounded ice is presently situated below sea level (Fretwell et al., 2013), including the extensive Recovery, Wilkes, and Aurora subglacial basins in East Antarctica.

evaluated with recourse to their ability to reproduce past ice sheet behavior and sea level change, in particular during warmer climate intervals, as constrained by geological and oceanographic evidence (Cook et al., 2013; Wilson et al., 2018; Young et al., 2011). Uncertainties and ambiguities associated with the geological proxies translate into uncertainties in projections of future ice sheet behavior (Oppenheimer et al., 2019).

A robust understanding of past AIS behavior is central to improving confidence in projections of future ice sheet contributions to global sea level rise. However, numerical models of past AISs have been restricted by a lack of knowledge of the temporal evolution of the bed topography, a boundary condition that exerts a fundamental influence on ice sheet dynamics (Gasson et al., 2015). The potential importance of changes in Antarctic bed topography for long-term ice sheet behavior has been previously noted (Colleoni et al., 2018; Gasson et al., 2016). These studies examined AIS dynamics at a single snapshot in time (the mid-Miocene) using an interpolation between an early reconstruction of paleotopography for the Eocene-Oligocene boundary (ca. 34 Myr ago) (Wilson et al., 2012) and the modern topography. However, Colleoni et al. (2018) noted that a lack of robust past topographic reconstructions results in a shortcoming in our understanding of the AIS response to past climatic evolution. Here, we seek to address this issue by quantifying the progressive change in AIS sensitivity due to topographic changes since AIS inception at the Eocene-Oligocene boundary using robustly constrained time-evolving reconstructions of past Antarctic topography that incorporate physical processes including erosion, tectonics, and isostatic feedbacks (Text S1 in the supporting information) (Paxman et al., 2019). Our aim is to quantify the progressively changing sensitivity of the AIS to climate and ocean forcing in an ice sheet model as a function of the evolving topography.

2. Methods

To investigate the influence of Antarctica's long-term bed topography evolution on AIS behavior, we performed ice sheet simulations using a numerical model with hybrid ice flow dynamics and formulations for marine ice shelf hydrofracture and ice cliff failure (Text S2) that has been used to model past, present, and future AISs (DeConto & Pollard, 2016; Gasson et al., 2016; Pollard et al., 2015).

The boundary conditions used in the ice sheet simulations were a modern bed topography data set recently updated to incorporate bed elevation data acquired since the Bedmap2 compilation (Fretwell et al., 2013; Paxman et al., 2019) (Figure 1) and four recently reconstructed paleotopographies (Figure S1) pertaining to the mid-Pliocene warm period (ca. 3.5 Ma), mid-Miocene climate transition (ca. 14 Ma), Oligocene-Miocene boundary (ca. 23 Ma), and Eocene-Oligocene boundary (ca. 34 Ma) (Paxman et al., 2019). These four time intervals correspond to periods of significant climatic and glacial change in Antarctica (Miller et al., 2020) and represent periods of warmer climate and elevated atmospheric CO_2 concentrations that have been used as analogs for future climate conditions (Burke et al., 2018; Gasson et al., 2016; Levy et al., 2016; Naish et al., 2001). The paleotopographies were reconstructed using geophysical methods and constrained using a range of independent geological data (Text S1) (Paxman et al., 2019). To examine the effect of the uncertainties associated with the paleotopographies, we ran our simulations on the "minimum," "median," and "maximum" reconstructions of Paxman et al. (2019) (Text S1) for each time interval. For simplicity, results displayed in this study pertain to the median paleotopographies, with the minimum and maximum models used to define error bounds where applicable.

For each bed topography, we performed the same three ice sheet-climate simulations (Text S3). The first involved the growth of an ice sheet on ice-free bed under "colder climate" conditions with preindustrial atmospheric CO_2 concentrations of 280 parts per million (ppm). The second involved the subsequent deglaciation of this ice sheet by changing to "warmer climate" conditions, involving a shift in orbital parameters (Text S3), an instantaneous increase in CO_2 concentrations to 500 ppm, and a uniform 5°C of ocean warming. The third simulation was identical to the second, but with an increase to "high CO_2" concentrations of 840 ppm. Warming experiments with a lower ocean warming of 2°C were also performed to assess the impact of ocean temperatures on modeled ice volume loss (Text S3). We ran the simulations for 10 kyr, by which point quasi-steady-state conditions were reached, and extracted the modeled ice sheet configuration, volume, and sea level equivalent. The sensitivity of the modeled ice sheet extent to ocean and climate perturbations is influenced by the particular physics of the ice sheet model. The model includes ice cliff failure and ice shelf hydrofracture (Text S2), which are recently proposed mechanisms for enhancing rapid marine ice sheet retreat (Pollard et al., 2015) that may be required to reproduce past sea level variability (DeConto & Pollard, 2016). These processes remain controversial (Clerc et al., 2019; Edwards et al., 2019; Robel & Banwell, 2019), and the retreat rate caused by marine ice cliff instability is poorly constrained. We therefore present ice sheet model results with and without these processes included.

We emphasize that the climate conditions used in these simulations are not intended to represent "true" climates that correspond to the specific ages of each paleotopography. The models are therefore not intended to reproduce "real" ice sheet configurations for any particular time interval but instead to assess the sensitivity of steady-state AIS extent and volume to the progressive evolution of bed topography in a widely used ice sheet model.

3. Results

3.1. Impact of Bed Topography on Ice Volume Loss

The simulations reveal that the amount of ice sheet thinning and retreat in response to climate and ocean warming shows a strong dependence on the bed topography (Figure 2). As the bed topography evolves from its ca. 34 Ma configuration to that of the present day, there is a systematic increase in the magnitude of AIS retreat and thinning that occurs in response to climate and ocean warming (Figure 2). In the warmer climate simulations, the topographically induced differences in modeled surface elevation/ice thickness within the Wilkes, Aurora and Recovery subglacial basins of East Antarctica are up to 3 km (Figures 2, 3, and S2). These subglacial basins have experienced significant (1–2 km) decreases in elevation since ca. 34 Ma (Figure S1). Modeled surface elevation and ice thickness differences in the interior of East Antarctica, where the landscape has remained relatively unmodified (Figure S1), are comparatively minor (<500 m) (Figures 2 and 3). The WAIS is almost entirely lost in both the 500 and 840 ppm deglaciation experiments (Figure 2) and does not evolve significantly in response to the lowering of West Antarctic bed topography by ~1 km since ca. 34 Ma (Figure S1).

The total warming-induced ice volume loss increases from 4.3×10^6 km^3 for the ca. 34 Ma topography to 6.1×10^6 km^3 for the modern topography for the 500 ppm simulation (Figure 4a), and from 4.3×10^6 km^3 to 9.7

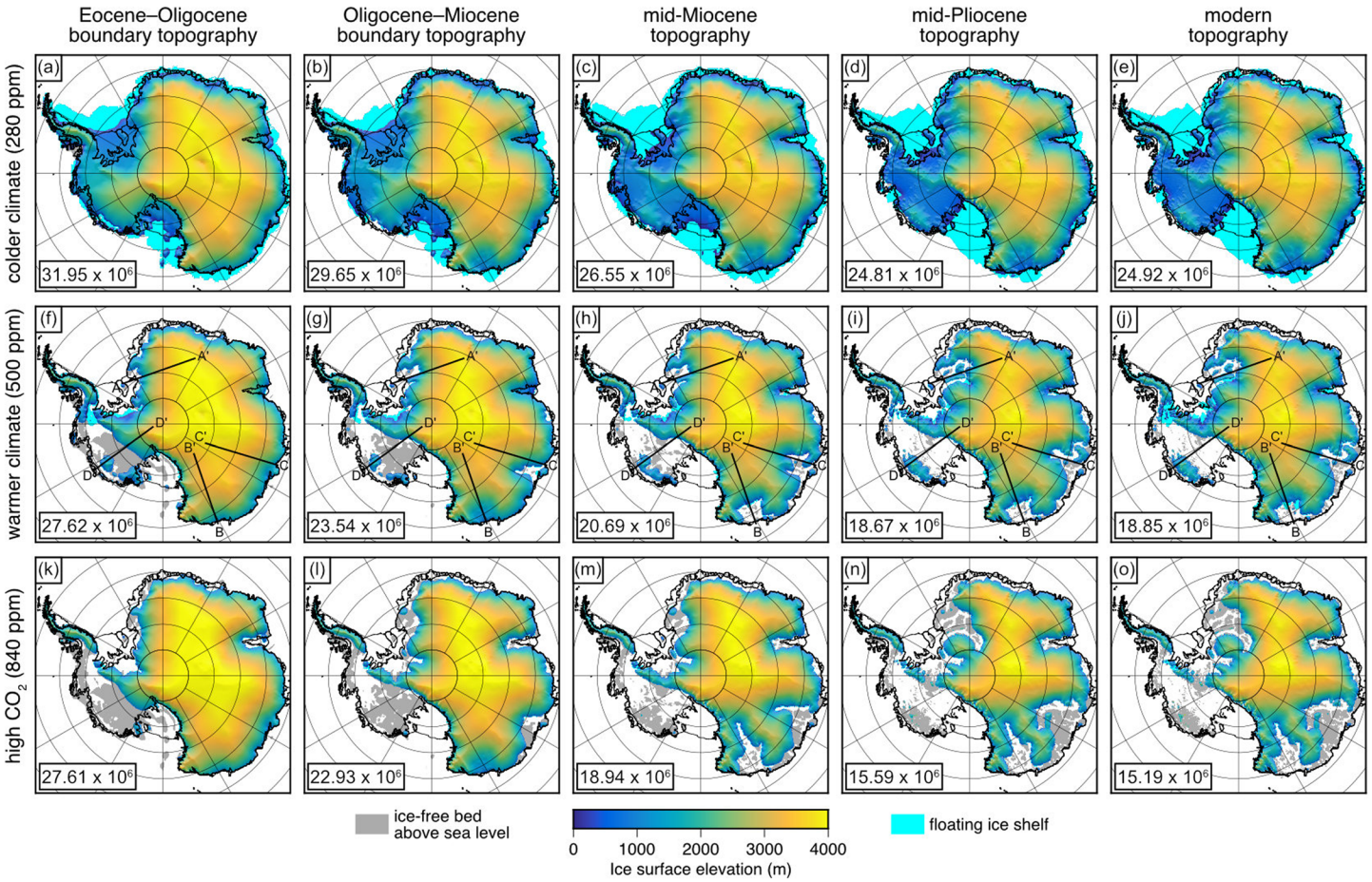

Figure 2. Ice sheet sensitivity to bed topography. The upper row (panels a–e) shows an ice sheet grown under a colder climate (pCO_2 = 280 ppm) on the four reconstructed median paleotopographies and the modern topography. The middle row (panels f–j) shows the ice sheet elevation on the same topographies following climate and ocean warming (pCO_2 = 500 ppm; 5°C ocean temperature rise). Profiles A-A′, B-B′, C-C′, and D-D′ are shown in Figure S2. The lower row (panels k–o) shows the ice sheet elevation following climate and ocean warming with a larger increase in pCO_2 to 840 ppm. Modeled total ice sheet volumes (in km^3) are given in each panel.

$\times 10^6$ km^3 for the 840 ppm simulation (Figure 4c; Table S1). The additional ice volume losses of 1.8×10^6 km^3 and 5.4×10^6 km^3 are equivalent to a global mean sea level rise of 2.6 and 10 m for the 500 and 840 ppm simulations, respectively (Figures 4b and 4d; Table S1; Text S2). The range of modeled ice volume loss between the minimum and maximum paleotopographies is largest for the oldest time slices (up to ~25% of the total; Figure 4), since these reconstructions are associated with the greatest uncertainty (Paxman et al., 2019). However, the trend of increased volume loss with the evolution of topography is consistently borne out despite this uncertainty (Figure 4).

Accounting for the difference in timespan between the different paleotopographies, the ice volume loss from the EAIS increases approximately linearly with the progressive evolution of topography for both the 500 and 840 ppm warming experiments (Figure 4). Differences in AIS volume loss between the 3.5 Ma and modern topographies are comparatively small, even showing a small decrease of 0.1×10^6 km^3 between these topographies in the 500 ppm simulation (Figure 4a). This decrease is caused by localized differences in interior ice thickness between the near-identical 3.5 Ma and modern topographies (Figure S1; Table S1). Although the volume lost from the WAIS appears to decrease with the evolution of the bed topography (Figure 4), this reflects a reduction in initial colder climate WAIS volume rather than a reduction in sensitivity to climate and ocean warming (Figure S3). Accounting for the fact that the initial ice sheets have different volumes (Figure S3), the proportion of the initial ice volume that is lost in the 840 ppm simulations shows a progressive increase from 13.5% (ca. 34 Ma) to 39.0% (modern) (Figure S4).

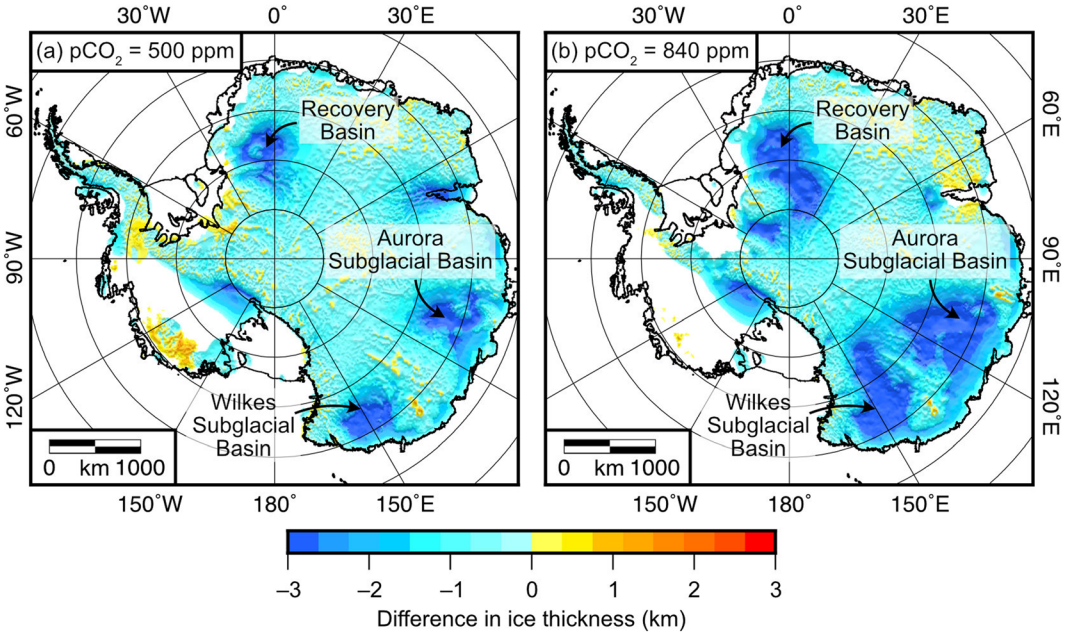

Figure 3. Dependence of modeled ice thickness on subglacial topography. (a) Difference in modeled ice thickness under warmer climate (pCO_2 = 500 ppm; 5°C ocean temperature rise) conditions between the simulations using the modern topography and the median Eocene-Oligocene boundary topography. (b) Difference in modeled ice thickness under high CO_2 (pCO_2 = 840 ppm; 5°C ocean temperature rise) conditions between the simulations using the modern topography and the median Eocene-Oligocene boundary topography. Positive values indicate thicker ice on the modern topography; negative values indicate thinner ice on the modern topography. White areas indicate absence of ice for both topographies.

There was negligible additional loss of ice volume when pCO_2 was increased to 840 ppm compared to 500 ppm for the ca. 34 and ca. 23 Ma topographies (Figure 4; Table S1). By contrast, the ca. 3.5 Ma and modern topographies showed a more appreciable difference in ice volume loss of up to 4.0×10^6 km^3 between the two warmer climate simulations, which is largely sourced from the EAIS (Figure 4; Table S1). For the older topographies, this lack of sensitivity arises because ice surface accumulation and loss via surface/basal melt and calving remain closely balanced after this additional pCO_2 increase (see section 3.2).

3.2. Mechanisms of Ice Volume Loss

In the warmer climate experiments, ice mass loss is driven primarily by marine ice cliff instability in regions of reverse-sloping bed, as well as calving and subice shelf melt (Figure S5). Up to 1,000 km of additional retreat of the ice margin into low-lying subglacial basins around the East Antarctic coast (Figures 2, 3, and S2) is enabled largely due to the enhanced marine instability caused by ice shelf hydrofracture and ice cliff failure. We found that 2°C of ocean warming resulted in very similar ice volume losses to the 5°C simulations, suggesting that 2°C of ocean warming combined with marine ice sheet instability is sufficient to cause the majority of the observed ice retreat. When these processes are switched off in the model (Figure S6), the shift to warmer climate (pCO_2 = 500 ppm) conditions causes an increase in ice volume of 0.9×10^6 km^3 for the ca. 34 Ma topography (due to increased surface accumulation exceeding ice mass loss; Figure S5). As the topography evolves toward the modern configuration, this small ice volume increase progressively shifts to an ice volume loss of 2.6×10^6 km^3 (Table S2).

The magnitudes of ice volume loss in the simulations that do not incorporate ice shelf hydrofracture and ice cliff failure are ~70% lower than the equivalent simulations that do include these processes. However, the relative increase in ice sheet sensitivity to climate and ocean forcing (and resulting additional volume loss) as the bed topography evolves toward its modern configuration is still observed (Table S2; Figure S6). While the most appropriate model physics for simulating ice sheet retreat under climate and ocean warming conditions remains debated (DeConto & Pollard, 2016; Edwards et al., 2019), the key finding of our study is that

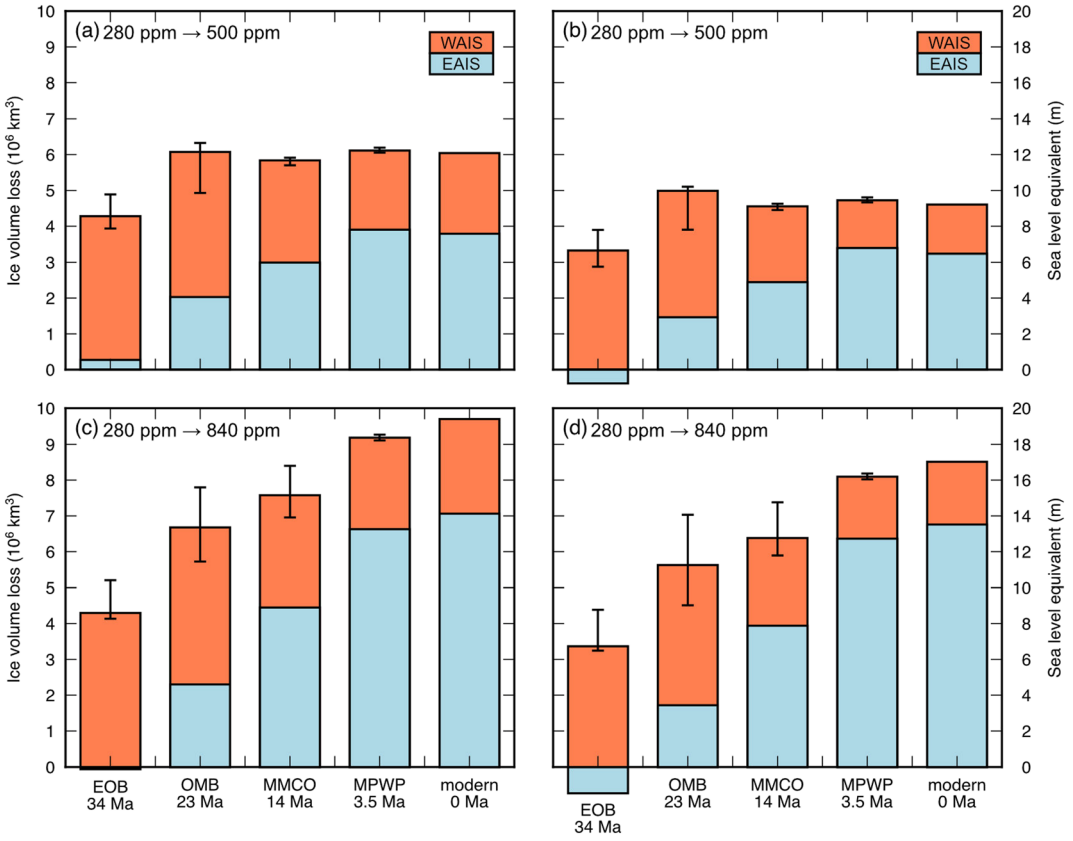

Figure 4. Ice volume loss and equivalent sea level rise in response to modeled climate and ocean warming for different bed topographies. (a) Ice volume lost following a change from colder climate (pCO_2 = 280 ppm) to warmer climate (pCO_2 increased to 500 ppm; 5°C ocean temperature rise) conditions on the different topographies. (b) Sea level equivalent of the ice volume lost shown in panel a. (c) Ice volume lost following a change from colder climate (pCO_2 = 280 ppm) to high CO_2 (pCO_2 increased to 840 ppm; 5°C ocean temperature rise) conditions on the different topographies. (d) Sea level equivalent of the ice volume lost shown in panel c. Ice volumes and sea level equivalents are separated into EAIS (blue) and WAIS (red) components. Bars situated below zero indicate a growth in ice volume and sea level equivalent. Colored bars show ice volumes and sea level equivalents for the median paleotopographies; vertical error bars show the total AIS ranges for the minimum and maximum end-member paleotopographies. Abbreviations: EOB = Eocene-Oligocene boundary; OMB = Oligocene-Miocene boundary; MMCT = mid-Miocene climate transition; MPWP = mid-Pliocene warm period.

changes in ice volume induced by simulated climate and ocean warming are strongly sensitive to, and modulated by, the bed topography boundary condition imposed upon the ice sheet model.

4. Discussion

Our results demonstrate that as the bed topography of Antarctica evolves from its early geometry toward modern-day elevations, the simulated AIS becomes progressively more sensitive to climate and ocean forcing. In our deglaciation experiments, this increased AIS sensitivity is expressed in terms of (a) a doubling in the total magnitude of ice volume loss (Figure 4) and (b) a threefold increase in the proportion of the initial ice volume that is lost in the "high CO_2" (840 ppm) simulations (Figure S4) when switching from the ca. 34 Ma topography to the modern topography. We note that our simplified experiments examine the steady-state ice sheet response to climate and ocean warming rather than transient behavior. Since the transient response has important implications for the rates of ice mass change (Stap et al., 2019), we highlight this as an important target for future ice sheet modeling studies using these paleotopographies. Furthermore, while we have focused on the effects of long-term continental-scale landscape evolution on AIS behavior, we note the potential importance of (i) smaller-scale variability in bed topography such as the presence of bedrock "bumps" or pinning points (Fürst et al., 2015; Matsuoka et al., 2015) and (ii)

shorter-term processes such as glacial isostatic adjustment (Barletta et al., 2018; Kingslake et al., 2018) for modifying ice sheet stability.

It was also recently demonstrated that continental shelf evolution has increased AIS sensitivity to climatic change (Colleoni et al., 2018). Because the topographic reconstructions used herein constrain continent-wide erosion, tectonics, and isostasy, we can further expand on this previous study and begin to assess the relative importance of these processes in controlling the time-evolving sensitivity of the AIS to climate and ocean forcing.

In our model experiments, EAIS volume loss is largely sourced from the Wilkes, Recovery, and Aurora subglacial basins and is primarily driven by ocean warming-induced marine ice cliff instability processes (Figures 2, 3, and S5). By comparing the processes responsible for landscape evolution within these basins (Paxman et al., 2019) to the patterns of modeled ice sheet retreat, we note that glacial erosion is primarily responsible for the additional retreat of the EAIS margin on the "younger" paleotopographies, with the effects of erosion partially offset by the consequent flexural uplift (Figure S7). We therefore attribute the observed increase in EAIS sensitivity within the near-coastal Wilkes, Recovery, and Aurora subglacial basins to the increase in the fraction of bed situated below sea level, and in particular the development and steepening of reverse bed slopes, driven by progressive erosion of the bed over geological time (Figure S1; Table S1). These subglacial basins have been highlighted as potentially key contributors to EAIS volume loss and sea level rise both in the past (Aitken et al., 2016; Cook et al., 2013; Young et al., 2011) and in the future (DeConto & Pollard, 2016; Golledge et al., 2017). Our results indicate that the long-term evolution of Antarctica's bed topography since ca. 34 Ma has contributed significantly to the enhanced sensitivity of these regions of the EAIS to climate and ocean forcing.

Although the three East Antarctic subglacial basins mentioned above appear to show a similar relationship between glacial erosion and increased ice sheet sensitivity, differences are observed in the spatial patterns of ice margin retreat. In the Recovery Basin, the ice margin preferentially retreats within a series of linear subglacial trough systems while ice persists on the adjacent highlands (Figure 2), whereas the Wilkes and Aurora Subglacial Basins exhibit more spatially uniform ice margin retreat (Figure 2). These contrasting patterns of retreat likely reflect the differing topographic and tectonic structure of the basins. The relief of the Recovery Basin is controlled by fault systems that separate deep subglacial troughs from linear highlands (Paxman et al., 2017) and appear to focus ice sheet retreat (Figure 2). By contrast, the Wilkes and Aurora Subglacial Basins are broader structures formed during, and subsequently influenced by, the long-term Proterozoic-Phanerozoic tectonic evolution of East Antarctica (Aitken et al., 2014; Ferraccioli et al., 2009). This illustrates how AIS behavior can be influenced by the geomorphic processes that have acted to modify the subglacial landscape since ice sheet inception and also by the preexisting crustal structure that has been established over the course of Antarctica's geological history.

In our ice sheet models, the time-evolving change in ice sheet sensitivity is primarily observed in the EAIS rather than the WAIS. In the West Antarctic Rift System, thermal subsidence has, alongside erosion, played a significant role in the lowering of bed elevations (Figure S7) (Wilson & Luyendyk, 2009), but the complex interplay between mantle dynamics, crustal deformation, thermal effects, erosion, sedimentation, and isostasy remains poorly constrained in paleotopography models due to a paucity of geological data. This in turn makes interpreting past WAIS dynamics particularly challenging. Ongoing and future acquisition of geophysical data sets (e.g., Tinto et al., 2019) and geological data from ocean and subice drilling (e.g., Coenen et al., 2020) may lead to significant advances in our understanding of the geological and topographic evolution of West Antarctica beyond what is currently captured by continental paleotopography models. Indeed, the ice sheet model results presented in this study highlight the importance of robust paleotopographic reconstructions for understanding past AIS behavior and sensitivity and continued improvement of these reconstructions through acquisition of datasets proximal and distal to the Antarctic continent is an important priority for future research.

5. Conclusions

We conclude that the sensitivity of the AIS to climate and ocean forcing has substantially increased as a result of the long-term evolution of Antarctica's subglacial landscape since ice sheet inception at the Eocene-Oligocene boundary (ca. 34 Ma). Furthermore, our findings highlight the role of bed topography

as a control on ice sheet behavior and demonstrate the importance of using a realistic suite of reconstructed paleotopographies to model past AISs and associated sea level changes with increased confidence. Our results also underline the importance of the low-lying Recovery, Wilkes, and Aurora subglacial basins of East Antarctica as potential areas of significant past and future ice volume loss (Cook et al., 2013; DeConto & Pollard, 2016; Golledge et al., 2017). The lowering of bed elevations within these basins has primarily been caused by the removal of material by glacial erosion (Jamieson et al., 2010; Paxman et al., 2019). The development of a bed geometry that amplifies the sensitivity of the AIS to climate and ocean forcing, and thereby its vulnerability to retreat, has therefore been driven largely by the ice sheet itself, suggesting that the AIS has become a victim of its own efficacy in shaping the underlying landscape.

Data Availability Statement

All paleotopographic reconstructions used in this study are available online (at https://doi.org/10.1016/j.palaeo.2019.109346). Ice sheet model outputs are available at the NERC/BAS Polar Data Centre (https://doi.org/10.5285/D67A07A8-BECC-419D-99F7-5578928461CA).

Acknowledgments

G. J. G. P. was funded by a Natural Environment Research Council UK studentship NE/L002590/1. E. G. W. G. is supported by a Royal Society University Research Fellowship. F. F.'s work on Antarctic bed topography was carried out within the framework of the 4-D Antarctica project funded by the European Space Agency. This research is a contribution to the Scientific Committee on Antarctic Research (SCAR) Past Antarctic Ice Sheet dynamics (PAIS) Scientific Research Program. The authors would like to acknowledge the support of the numerous members of SCAR and PAIS who were instrumental in the development of this research. We would also like to thank the two anonymous reviewers for their constructive comments, which helped improve the final manuscript.

References

Aitken, A. R. A., Roberts, J. L., van Ommen, T. D., Young, D. A., Golledge, N. R., Greenbaum, J. S., et al. (2016). Repeated large-scale retreat and advance of Totten Glacier indicated by inland bed erosion. *Nature*, *533*(7603), 385–389. https://doi.org/10.1038/nature17447

Aitken, A. R. A., Young, D. A., Ferraccioli, F., Betts, P. G., Greenbaum, J. S., Richter, T. G., et al. (2014). The subglacial geology of Wilkes Land, East Antarctica. *Geophysical Research Letters*, *41*, 2390–2400. https://doi.org/10.1002/2014GL059405

Barletta, V. R., Bevis, M., Smith, B. E., Wilson, T., Brown, A., Bordoni, A., et al. (2018). Observed rapid bedrock uplift in Amundsen Sea Embayment promotes ice-sheet stability. *Science*, *360*(6395), 1335–1339. https://doi.org/10.1126/science.aao1447

Burke, K. D., Williams, J. W., Chandler, M. A., Haywood, A. M., Lunt, D. J., & Otto-Bliesner, B. L. (2018). Pliocene and Eocene provide best analogs for near-future climates. *Proceedings of the National Academy of Sciences of the United States of America*, *115*(52), 13,288–13,293. https://doi.org/10.1073/pnas.1809600115

Clerc, F., Minchew, B. M., & Behn, M. D. (2019). Marine ice cliff instability mitigated by slow removal of ice shelves. *Geophysical Research Letters*, *46*, 12,108–12,116. https://doi.org/10.1029/2019GL084183

Coenen, J. J., Scherer, R., Baudoin, P., Warny, S., Castañeda, I. S., & Askin, R. (2020). Paleogene marine and terrestrial development of the West Antarctic Rift System. *Geophysical Research Letters*, *47*, e2019GL085281. https://doi.org/10.1029/2019GL085281

Colleoni, F., De Santis, L., Montoli, E., Olivo, E., Sorlien, C. C., Bart, P. J., et al. (2018). Past continental shelf evolution increased Antarctic ice sheet sensitivity to climatic conditions. *Scientific Reports*, *8*(1), 11323. https://doi.org/10.1038/s41598-018-29718-7

Cook, C. P., Van De Flierdt, T., Williams, T., Hemming, S. R., Iwai, M., Kobayashi, M., et al. (2013). Dynamic behaviour of the East Antarctic ice sheet during Pliocene warmth. *Nature Geoscience*, *6*(9), 765–769. https://doi.org/10.1038/ngeo1889

DeConto, R. M., & Pollard, D. (2016). Contribution of Antarctica to past and future sea-level rise. *Nature*, *531*(7596), 591–597. https://doi.org/10.1038/nature17145

Edwards, T. L., Brandon, M. A., Durand, G., Edwards, N. R., Golledge, N. R., Holden, P. B., et al. (2019). Revisiting Antarctic ice loss due to marine ice-cliff instability. *Nature*, *566*(7742), 58–64. https://doi.org/10.1038/s41586-019-0901-4

Ferraccioli, F., Armadillo, E., Jordan, T., Bozzo, E., & Corr, H. (2009). Aeromagnetic exploration over the East Antarctic Ice Sheet: A new view of the Wilkes Subglacial Basin. *Tectonophysics*, *478*(1–2), 62–77. https://doi.org/10.1016/j.tecto.2009.03.013

Forsberg, R., Olesen, A. V., Ferraccioli, F., Jordan, T. A., Matsuoka, K., Zakrajsek, A., et al. (2018). Exploring the Recovery Lakes region and interior Dronning Maud Land, East Antarctica, with airborne gravity, magnetic and radar measurements. *Geological Society of London, Special Publication*, *461*. https://doi.org/10.1144/SP461.17

Fretwell, P., Pritchard, H. D., Vaughan, D. G., Bamber, J. L., Barrand, N. E., Bell, R., et al. (2013). Bedmap2: Improved ice bed, surface and thickness datasets for Antarctica. *The Cryosphere*, *7*(1), 375–393. https://doi.org/10.5194/tc-7-375-2013

Fürst, J. J., Durand, G., Gillet-Chaulet, F., Merino, N., Tavard, L., Mouginot, J., et al. (2015). Assimilation of Antarctic velocity observations provides evidence for uncharted pinning points. *The Cryosphere*, *9*(4), 1427–1443. https://doi.org/10.5194/tc-9-1427-2015

Gasson, E., DeConto, R. M., & Pollard, D. (2015). Antarctic bedrock topography uncertainty and ice sheet stability. *Geophysical Research Letters*, *42*, 5372–5377. https://doi.org/10.1002/2015GL064322

Gasson, E., DeConto, R. M., Pollard, D., & Levy, R. H. (2016). Dynamic Antarctic ice sheet during the early to mid-Miocene. *Proceedings of the National Academy of Sciences*, *113*(13), 3459–3464. https://doi.org/10.1073/pnas.1516130113

Golledge, N. R., Kowalewski, D. E., Naish, T. R., Levy, R. H., Fogwill, C. J., & Gasson, E. G. W. (2015). The multi-millennial Antarctic commitment to future sea-level rise. *Nature*, *526*(7573), 421–425. https://doi.org/10.1038/nature15706

Golledge, N. R., Levy, R. H., McKay, R. M., & Naish, T. R. (2017). East Antarctic ice sheet most vulnerable to Weddell Sea warming. *Geophysical Research Letters*, *44*, 2343–2351. https://doi.org/10.1002/2016GL072422

Jamieson, S. S. R., Sugden, D. E., & Hulton, N. R. J. (2010). The evolution of the subglacial landscape of Antarctica. *Earth and Planetary Science Letters*, *293*(1–2), 1–27. https://doi.org/10.1016/j.epsl.2010.02.012

Jordan, T. A., Martin, C., Ferraccioli, F., Matsuoka, K., Corr, H., Forsberg, R., et al. (2018). Anomalously high geothermal flux near the South Pole. *Scientific Reports*, *8*(1), 16785. https://doi.org/10.1038/s41598-018-35182-0

Kingslake, J., Scherer, R. P., Albrecht, T., Coenen, J., Powell, R. D., Reese, R., et al. (2018). Extensive retreat and re-advance of the West Antarctic Ice Sheet during the Holocene. *Nature*, *558*(7710), 430–434. https://doi.org/10.1038/s41586-018-0208-x

Levy, R., Harwood, D., Florindo, F., Sangiorgi, F., Tripati, R., von Eynatten, H., et al. (2016). Antarctic ice sheet sensitivity to atmospheric CO_2 variations in the early to mid-Miocene. *Proceedings of the National Academy of Sciences of the United States of America*, *113*(13), 3453–3458. https://doi.org/10.1073/pnas.1516030113

Matsuoka, K., Hindmarsh, R. C. A., Moholdt, G., Bentley, M. J., Pritchard, H. D., Brown, J., et al. (2015). Antarctic ice rises and rumples: Their properties and significance for ice-sheet dynamics and evolution. *Earth-Science Reviews*, *150*, 724–745. https://doi.org/10.1016/j.earscirev.2015.09.004

Mercer, J. H. (1978). West Antarctic ice sheet and CO_2 greenhouse effect: A threat of disaster. *Nature*, *104*(25), 10,335–10,339. https://doi.org/10.1073/pnas.0703993104

Miller, K. G., Browning, J. V., Schmelz, W. J., Kopp, R. E., Mountain, G. S., & Wright, J. D. (2020). Cenozoic sea-level and cryospheric evolution from deep-sea geochemical and continental margin records. *Science Advances*, *6*(20), eaaz1346. https://doi.org/10.1126/sciadv.aaz1346

Morlighem, M., Rignot, E., Binder, T., Blankenship, D., Drews, R., Eagles, G., et al. (2020). Deep glacial troughs and stabilizing ridges unveiled beneath the margins of the Antarctic ice sheet. *Nature Geoscience*, *13*(2), 132–137. https://doi.org/10.1038/s41561-019-0510-8

Naish, T. R., Woolfe, K. J., Barrett, P. J., Wilson, G. S., Atkins, C., Bohaty, S. M., et al. (2001). Orbitally induced oscillations in the East Antarctic ice sheet at the Oligocene/Miocene boundary. *Nature*, *413*(6857), 719–723. https://doi.org/10.1038/35099534

Oppenheimer, M., Glavovic, B. C., Hinkel, J., van de Wal, R., Magnan, A. K., Abd-Elgawad, A., et al. (2019). Sea level rise and implications for low-lying islands, coasts and communities. In H.-O. Pörtner, et al. (Eds.), *IPCC Special Report on the Ocean and Cryosphere in a Changing Climate*. Cambridge, UK: Cambridge University Press.

Paxman, G. J. G., Jamieson, S. S. R., Ferraccioli, F., Bentley, M. J., Forsberg, R., Ross, N., et al. (2017). Uplift and tilting of the Shackleton Range in East Antarctica driven by glacial erosion and normal faulting. *Journal of Geophysical Research: Solid Earth*, *122*, 2390–2408. https://doi.org/10.1002/2016JB013841

Paxman, G. J. G., Jamieson, S. S. R., Hochmuth, K., Gohl, K., Bentley, M. J., Leitchenkov, G., & Ferraccioli, F. (2019). Reconstructions of Antarctic topography since the Eocene-Oligocene boundary. *Palaeogeography Palaeoclimatology Palaeoecology*, *535*, 109346. https://doi.org/10.1016/j.palaeo.2019.109346

Pollard, D., DeConto, R. M., & Alley, R. B. (2015). Potential Antarctic Ice Sheet retreat driven by hydrofracturing and ice cliff failure. *Earth and Planetary Science Letters*, *412*, 112–121. https://doi.org/10.1016/j.epsl.2014.12.035

Rignot, E., Mouginot, J., Scheuchl, B., Van Den Broeke, M., Van Wessem, M. J., & Morlighem, M. (2019). Four decades of Antarctic ice sheet mass balance from 1979–2017. *Proceedings of the National Academy of Sciences of the United States of America*, *116*(4), 1095–1103. https://doi.org/10.1073/pnas.1812883116

Robel, A. A., & Banwell, A. F. (2019). A speed limit on ice shelf collapse through hydrofracture. *Geophysical Research Letters*, *46*, 12,092–12,100. https://doi.org/10.1029/2019GL084397

Schoof, C. (2007). Ice sheet grounding line dynamics: Steady states, stability, and hysteresis. *Journal of Geophysical Research*, *112*, F03S28. https://doi.org/10.1029/2006JF000664

Slater, T., Shepherd, A., McMillan, M., Muir, A., Gilbert, L., Hogg, A. E., et al. (2018). A new digital elevation model of Antarctica derived from CryoSat-2 altimetry. *The Cryosphere*, *12*(4), 1551–1562. https://doi.org/10.5194/tc-2017-223

Stap, L. B., Sutter, J., Knorr, G., Stärz, M., & Lohmann, G. (2019). Transient variability of the Miocene Antarctic ice sheet smaller than equilibrium differences. *Geophysical Research Letters*, *46*, 4288–4298. https://doi.org/10.1029/2019GL082163

Thomas, R. H. (1979). The dynamics of marine ice sheets. *Journal of Glaciology*, *24*(90), 167–177. https://doi.org/10.1017/S0022143000014726

Tinto, K. J., Padman, L., Siddoway, C. S., Springer, S. R., Fricker, H. A., Das, I., et al. (2019). Ross Ice Shelf response to climate driven by the tectonic imprint on seafloor bathymetry. *Nature Geoscience*, *12*(6), 441–449. https://doi.org/10.1038/s41561-019-0370-2

Wilson, D. J., Bertram, R. A., Needham, E. F., van de Flierdt, T., Welsh, K. J., McKay, R. M., et al. (2018). Ice loss from the East Antarctic Ice Sheet during late Pleistocene interglacials. *Nature*, *561*(7723), 383–386. https://doi.org/10.1038/s41586-018-0501-8

Wilson, D. S., Jamieson, S. S. R., Barrett, P. J., Leitchenkov, G., Gohl, K., & Larter, R. D. (2012). Antarctic topography at the Eocene-Oligocene boundary. *Palaeogeography Palaeoclimatology Palaeoecology*, *335–336*, 24–34. https://doi.org/10.1016/j.palaeo.2011.05.028

Wilson, D. S., & Luyendyk, B. P. (2009). West Antarctic paleotopography estimated at the Eocene-Oligocene climate transition. *Geophysical Research Letters*, *36*, L16302. https://doi.org/10.1029/2009GL039297

Young, D. A., Wright, A. P., Roberts, J. L., Warner, R. C., Young, N. W., Greenbaum, J. S., et al. (2011). A dynamic early East Antarctic Ice Sheet suggested by ice-covered fjord landscapes. *Nature*, *474*(7349), 72–75. https://doi.org/10.1038/nature10114